

Extensive Genetic Differentiation between Homomorphic Sex Chromosomes in the Mosquito Vector, *Aedes aegypti*

Albin Fontaine^{1,2,3,4}, Igor Filipović⁵, Thanyalak Fansiri⁶, Ary A. Hoffmann⁵, Changde Cheng⁷, Mark Kirkpatrick⁷, Gordana Rašić^{5,*}, and Louis Lambrechts^{1,3,*}

¹Department of Genomes and Genetics, Insect-Virus Interactions Group, Institut Pasteur, Paris, France

²Département des Maladies Infectieuses, Unité de Parasitologie et Entomologie, Institut de Recherche Biomédicale des Armées, Marseille, France

³Centre National de la Recherche Scientifique, URA 3012, Paris, France

⁴Aix Marseille Université, UM63, CNRS 7278, IRD 198, INSERM 1095, AP-HM, IHU-Méditerranée Infection, France

⁵Pest and Environmental Adaptation Research Group, School of BioSciences and Bio21 Institute, Faculty of Science, The University of Melbourne, Victoria, Australia

⁶Department of Entomology, Armed Forces Research Institute of Medical Sciences, Bangkok, Thailand

⁷Department of Integrative Biology, University of Texas, Austin

*Corresponding authors: E-mails: rasic.gordana@gmail.com; louis.lambrechts@pasteur.fr.

Accepted: August 31, 2017

Data deposition: Data from this project have been deposited at the NCBI Sequence Read Archive under accession numbers SRP116065, SRX1970106-SRX1970108 and SRX2248021.

Abstract

Mechanisms and evolutionary dynamics of sex-determination systems are of particular interest in insect vectors of human pathogens like mosquitoes because novel control strategies aim to convert pathogen-transmitting females into nonbiting males, or rely on accurate sexing for the release of sterile males. In *Aedes aegypti*, the main vector of dengue and Zika viruses, sex determination is governed by a dominant male-determining locus, previously thought to reside within a small, nonrecombining, sex-determining region (SDR) of an otherwise homomorphic sex chromosome. Here, we provide evidence that sex chromosomes in *Ae. aegypti* are genetically differentiated between males and females over a region much larger than the SDR. Our linkage mapping intercrosses failed to detect recombination between X and Y chromosomes over a 123-Mbp region (40% of their physical length) containing the SDR. This region of reduced male recombination overlapped with a smaller 63-Mbp region (20% of the physical length of the sex chromosomes) displaying high male–female genetic differentiation in unrelated wild populations from Brazil and Australia and in a reference laboratory strain originating from Africa. In addition, the sex-differentiated genomic region was associated with a significant excess of male-to-female heterozygosity and contained a small cluster of loci consistent with Y-specific null alleles. We demonstrate that genetic differentiation between sex chromosomes is sufficient to assign individuals to their correct sex with high accuracy. We also show how data on allele frequency differences between sexes can be used to estimate linkage disequilibrium between loci and the sex-determining locus. Our discovery of large-scale genetic differentiation between sex chromosomes in *Ae. aegypti* lays a new foundation for mapping and population genomic studies, as well as for mosquito control strategies targeting the sex-determination pathway.

Key words: *Aedes aegypti*, sex chromosome, sex-linked alleles, RAD markers, WGS.

Introduction

Understanding the underlying mechanisms and evolutionary dynamics of sex determination in mosquitoes is of particular interest as new strategies for controlling mosquito-borne diseases aim to convert pathogen-transmitting females into

nonbiting males (Hall et al. 2015), or rely on accurate sexing for the release of sterile males (Eckermann et al. 2014; Gilles et al. 2014). Sex determination in mosquitoes and other dipterans is under the control of a gene regulation cascade that relies on alternative splicing of genes expressed in both males

and females (Salz 2011). There is a great deal of variation across dipteran species, and even between populations of the same species, in how this cascade is initiated (Bopp et al. 2014). The master switch at the top of the cascade in drosophilids is the number of X chromosomes, whereas in tephritids, houseflies, and mosquitoes it is a dominant male-determining factor (Kaiser and Bachtrog 2010; Vicoso and Bachtrog 2015).

In *Aedes* and *Culex* mosquitoes, the male-determining locus is located on a morphologically undifferentiated (homomorphic) sex chromosome, which is considered the ancestral state of mosquito sex chromosomes (Toups and Hahn 2010). In contrast, the malarial mosquitoes (Anophelinae) have acquired fully morphologically differentiated (heteromorphic) X and Y chromosomes (Toups and Hahn 2010). Why heteromorphy of sex chromosomes evolved in some mosquito lineages but not others remains unclear. Evolutionary models suggest progression of autosomes into heteromorphic sex chromosomes after the acquisition of a sex-determining locus (Charlesworth 1996; Charlesworth and Charlesworth 2000). According to these models, the selective advantage of linkage between sex-determining genes and sexually antagonistic genes promotes initial suppression of recombination between homologous chromosomes, followed by expansion of the nonrecombining region (Rice 1987). An evolving pair of neo-sex chromosomes further differentiates through changes in gene content, gene decay and epigenetic modifications (Bachtrog 2013). Yet, recent analyses of fly genomes revealed a striking diversity of evolutionary trajectories where sex chromosomes have been gained, lost, replaced, and rearranged multiple times over dipteran evolutionary history (Kaiser and Bachtrog 2010; Vicoso and Bachtrog 2015).

Aedes aegypti, the main vector of dengue, Zika, yellow fever, and chikungunya viruses worldwide, has homomorphic sex chromosomes like other Culicinae (Toups and Hahn 2010). Genetic evidence suggests that the male-determining locus resides in a nonrecombining, sex-determining region (SDR) of chromosome 1 (Toups and Hahn 2010). Motara and Rai (1978) proposed a nomenclature to define the copy of chromosome 1 with the M locus as the M chromosome, and the copy without the M locus as the m chromosome. Thereafter, we follow the standard terminology and refer to the m and M chromosomes as X and Y chromosomes, respectively. Motara and Rai also noticed some cytological differences consistent with differentiation of the SDR between the X and Y chromosomes of *Ae. aegypti* (Motara and Rai 1978). However, fine details of chromosomal features have been elusive due to problems in producing high-quality, easily spreadable polytene chromosomes in *Ae. aegypti* (Timoshevskiy et al. 2013).

Availability of a reference genome sequence (Nene et al. 2007) and affordable high-throughput sequencing technologies have opened new avenues to characterize genomic features in *Ae. aegypti*. Produced nearly 10 years ago, the *Ae. aegypti* reference genome sequence encompasses 1.39 billion

base pairs (Gbp) fragmented in over 4,700 scaffolds (Nene et al. 2007) that were recently assembled into end-to-end chromosomes by chromosome conformation capture (Dudchenko et al. 2017). Prior to this chromosome-wide assembly, linkage mapping using restriction site-associated DNA sequencing (RADseq) and physical mapping by fluorescent in situ hybridization (FISH) with metacentric chromosome preparations were used to produce partial assemblies, with up to two thirds of the genome sequence assigned to distinct chromosomes (Timoshevskiy et al. 2013; Juneja et al. 2014). Recent comparative genomic analyses suggested a particularly dynamic evolution of sex chromosomes that contain synteny blocks with the X and 2R chromosome arms of *Anopheles gambiae* (Timoshevskiy et al. 2014).

The homomorphy of *Ae. aegypti* sex chromosomes was also inferred from genome-wide sequencing coverage differences between males and females (Vicoso and Bachtrog 2015). Because females have two copies of the X chromosome and males have only one, X-specific scaffolds are expected to display about half the depth of sequencing coverage in males compared with females. Vicoso and Bachtrog (2015) did not find a significant difference in depth of coverage between *Ae. aegypti* males and females when analyzing paired-end Illumina reads from whole-genome sequencing (WGS) libraries. This indicated that the Y-chromosome sequences are not sufficiently divergent from the X-chromosome sequences to preclude their successful alignment to the reference scaffolds, thus supporting the existence of undifferentiated sex chromosomes in *Ae. aegypti*. Hall and colleagues (2014) used a similar approach called the chromosome quotient method to identify the male-determining gene(s) within the SDR, but failed to do so when using the current *Ae. aegypti* genome sequence. Instead, they identified the male-determining gene *Nix* (Hall et al. 2015) and male-biased sequences primarily found in the male genome, such as the gene *myo-sex* (Hall et al. 2014), from transcriptomic data, expressed sequence tags and unassembled bacterial artificial chromosomes.

The overall conclusions from the previous studies are that: 1) the SDR in *Ae. aegypti* occupies a small region that maps to band 1q21 of chromosome 1, 2) regions near the SDR (including *myo-sex*) show low levels of recombination with the X chromosome (Hall et al. 2014), and 3) most of chromosome 1 recombines in an autosome-like fashion thereby maintaining the overall homomorphy. Also, the current genome sequence is considered largely uninformative when looking for sequences primarily found in the male genome (Hall et al. 2014, 2015).

Here, we provide compelling genetic evidence that, despite apparent homomorphy, sex chromosomes in *Ae. aegypti* are genetically differentiated over a region much larger than the nonrecombining SDR. Our linkage mapping experiments failed to detect recombination in F₁ males over a 123-million-base-pair (Mbp) region of chromosome 1, spanning from position 87 Mbp to position 210 Mbp and representing about 40% of its physical length. Analyses of genome-wide

variation in the unrelated laboratory strain (Liverpool) used to generate the current reference genome sequence, as well as in wild *Ae. aegypti* populations, revealed substantial male–female genetic differentiation in a smaller 63-Mbp region spanning from position 148 Mbp to position 211 Mbp and representing about 20% of the physical length of the sex chromosomes. A small cluster of loci located inside this region displayed genotypic patterns consistent with Y-specific null alleles. We further show that genetic differentiation between sex chromosomes is sufficient to accurately assign individuals to their phenotypic sex. We also demonstrate that allele frequency differences between males and females can be used to estimate linkage disequilibrium (LD) with the SDR. Our results lay a new foundation for the mapping and population genomic studies in *Ae. aegypti*, and for the control strategies that rely on accurate sexing and sex reversal in this important mosquito vector.

Materials and Methods

Mosquito Samples for Laboratory Crosses

Two independent laboratory crosses were carried out with wild-type *Ae. aegypti* mosquitoes originally collected in February 2011 from Kamphaeng Phet, Thailand. Cross #1 was an F₂ intercross created with a single virgin male from one isofemale line and a virgin female from another isofemale line. Both isofemale lines were derived from wild *Ae. aegypti* founders from Thailand collected as eggs using ovitraps as previously described (Fansiri et al. 2013). Prior to the cross, the lines were maintained in the laboratory by mass sib-mating and collective oviposition until the 19th generation. This was done to increase homozygosity and maximize the number of informative markers for our linkage mapping design. A total of 22 males and 22 females from the Cross #1 F₂ progeny were used to generate a linkage map and subsequently map the sex-determining locus. Cross #2 was an F₂ intercross between a pair of field-collected mosquito founders from Thailand (Fansiri et al. 2013). Adults were maintained in an insectary under controlled conditions (28 ± 1 °C, 75 ± 5% relative humidity and 12:12 h light–dark cycle). The male and female of each mating pair were chosen from different collection sites to avoid sampling siblings (Apostol et al. 1994; Rašić et al. 2014, 2016). Egg batches from the same F₀ female were merged to obtain a pool of F₁ eggs and F₂ progeny was produced by mass sib-mating and collective oviposition of the F₁ offspring (supplementary file 1E, Supplementary Material online). A total of 197 females of the Cross #2 F₂ progeny were used to generate a linkage map.

Field Samples for Population Genomic Analyses

Field-caught *Ae. aegypti* samples from Rio de Janeiro, Brazil and Queensland, Australia were analyzed. Samples of 62 adult mosquitoes from Australia were caught using

Biogents sentinel traps set up in Gordonvale (17 females and 17 males) and Townsville (14 females and 14 males), Queensland in January 2014 (Rašić et al. 2016). Adults were identified as males or females based on the sexually dimorphic antennae and external genitalia structure (Becker 2003). Mosquitoes from Rio de Janeiro, Brazil were collected from ovitraps in November–December 2011 (Rašić et al. 2015). Larvae were reared until the third instar in an insectary under controlled conditions (25 ± 1 °C, 80 ± 10% relative humidity and 12:12 h light–dark cycle). Only one individual per ovitrap was retained to avoid analyzing siblings. Sex of each individual was determined based on the presence or absence of the highly male-biased sequence *myo-sex* (Hall et al. 2014) and confirmed with two additional male-specific sequences that were identified in this study (supplementary file 1A and C, Supplementary Material online). The final data set from Brazil consisted of 66 mosquitoes (32 females and 34 males).

DNA Extraction

Mosquito genomic DNA was extracted using the NucleoSpin 96 Tissue Core Kit (Macherey-Nagel, Düren, Germany). To obtain a sufficient amount of DNA for the parental males from the laboratory crossings, whole-genome amplification was performed by multiple displacement amplification using the Repli-g Mini kit (Qiagen, Hilden, Germany). All DNA concentrations were measured with Qubit fluorometer and Quant-iT dsDNA Assay kit (Life technologies, Paisley, UK).

Double-Digest RADseq Library Generation

An adaptation of the original double-digest restriction-site associated DNA sequencing (ddRADseq) protocol (Peterson et al. 2012) was used as previously described (Rasic et al. 2014). Briefly, 500 ng of genomic DNA from each mosquito was used for the mapping samples, and 100 ng for the field-collected samples. DNA was digested in with *NlaIII* and *MluCI* restriction enzymes (New England Biolabs, Herts, UK), for 3 h at 37 °C. Cleaned digestions were ligated to the modified Illumina P1 and P2 adapters with overhangs complementary to *NlaIII* and *MluCI* cutting sites, respectively. Each mosquito was uniquely labeled with a combination of P1 and P2 barcodes. Ligation reactions were incubated at 16 °C overnight and heat inactivated. Adapter ligated DNA fragments from all individuals were then pooled and cleaned with 1.5× bead solution. Size selection of fragments between 350–440 base pairs (bp) for the laboratory crosses or 300–450 bp for the field populations was performed using a Pippin-Prep 2% gel cassette (Sage Sciences, Beverly, MA, USA). Finally, 1 μl of the size-selected DNA was used as a template in a 10-μl PCR reaction. To reduce PCR duplicates bias, eight PCR reactions were run in parallel, pooled, and cleaned to make the final library. Final libraries were quantified by quantitative PCR using the QPCR NGS Library Quantification Kit (Agilent technologies, Palo Alto, CA, USA). For the mapping crosses, libraries

spiked with 15% PhiX were sequenced in paired-end on an Illumina NextSeq 500 platform using a 150-cycle chemistry (Illumina, San Diego, CA, USA) (NCBI SRA accession number SRP116065). For the field populations, four ddRADseq libraries spiked with 10% PhiX were sequenced in paired-end on an Illumina HiSeq 2000 platform with a 100-cycle chemistry (NCBI SRA accession numbers SRX1970106-SRX1970108, SRX2248021).

Bioinformatics Processing and Genotype Calling

A previously developed bash script pipeline (Rasic et al. 2014) was used to process raw sequence reads. Briefly, the DDemux program was used for demultiplexing fastq files according to the P1 and P2 barcodes combinations. Sequences were filtered with FASTX-Toolkit, discarding the reads with Phred scores < 25. Reads were trimmed to 90 bp (HiSeq platform) and 140 bp (NextSeq platform) on both P1 and P2 ends. Reads were then aligned to the reference *Ae. aegypti* genome (AaegL1, February 2013) (Nene et al. 2007) using Bowtie version 0.12.7 (Langmead et al. 2009). Parameters for the ungapped alignment included a maximum of three mismatches allowed in the seed, suppression of alignments if more than one reportable alignment exists, and a “try-hard” option to find valid alignments. Aligned Bowtie output files were imported into the Stacks pipeline (Catchen et al. 2011, 2013).

A catalogue of RAD loci used for single nucleotide polymorphism (SNP) discovery was created using the ref_map.pl pipeline in Stacks version 1.19 (Catchen et al. 2011, 2013). A RAD locus was generated with a minimum of five reads. For the mapping crosses, the “genotypes” module was used to export F₂ mosquito genotypes for all markers homozygous for alternative alleles in the F₀ parents (i.e., homozygous AA in the F₀ male and homozygous BB in the F₀ female) with a sequencing depth $\geq 12 \times$ in $\geq 60\%$ of the mapping population, to minimize the risk of false homozygous calls.

AaegL1 genomic coordinates were translated into the recently published chromosome-wide AaegL4 assembly coordinates (Dudchenko et al. 2017). The AaegL1 assembly was blasted using blastn v2.6.0 against the AaegL4 assembly with default parameters, except a word size of 1,000 bp and a percentage identity of 100% between query and subject sequences. The genomic coordinates of each marker were translated based on the blast output file using an in-house awk script that accounted for potential fragment inversions between the two assemblies.

Linkage Map Construction

A comprehensive linkage map based on recombination fractions among RAD markers in the F₂ generation was constructed using the R package OneMap v2.0-3 (Margarido et al. 2007). Marker positions on the chromosome-wide AaegL4 assembly facilitated the assignment of markers to a linkage group and their respective ordering. Following the selection of markers for

which the parents were homozygous for alternative alleles, in Cross #1 every independent marker was expected to segregate in the F₂ mapping population at a frequency of 25% for homozygous genotypes (AA and BB) and of 50% for heterozygous genotypes (AB) when considering both males and females together. A χ^2 test was used to filter out markers based on deviations of the observed genotype frequencies in the F₂ progeny from the Mendelian segregation ratios expected for autosomal loci. Fully sex-linked markers are expected to segregate in F₂ females with equal frequency (50%) of AB and BB genotypes, because the F₀ paternal AA genotype only occurs in F₂ males (supplementary file 1D, Supplementary Material online). Reciprocally, fully sex-linked markers in F₂ males are expected to lack F₀ maternal BB genotypes.

Cross #2 could only be analyzed as a classical F₂ intercross design for autosomal linkage groups because only females were genotyped. Markers located on autosomes were filtered out based on deviations from expected Mendelian segregation ratios as described above. Markers on chromosome 1 were included if they had heterozygous genotype (AB) frequencies inside the 40–60% range and F₀ maternal genotype (BB) frequencies inside the 5–65% range. These arbitrary limits for initial marker selection were largely permissive for pseudo-autosomal markers segregating according to theoretical proportions (0–25% AA: 50% AB: 25–50% BB). To our knowledge, there is no linkage analysis method readily available to deal with such sex-specific deviations in genotype segregation ratios. Linkage analysis in Cross #2 was therefore restricted to chromosomes 2 and 3.

Recombination fractions between all pairs of selected markers were estimated using the rf.2pts function with default parameters. Because sex-specific recombination rates cannot be estimated with an F₂ cross design, a sex-averaged recombination rate was estimated. Markers linked with a minimum LOD score of 13 and 25 for Cross #1 and Cross #2, respectively, were assigned to the same linkage group and unlinked markers were removed from further analysis. Linkage groups were assigned to the three distinct *Ae. aegypti* chromosomes based on the physical coordinates of the chromosome-wide AaegL4 assembly.

Recombination fractions were converted into genetic distances in centiMorgans (cM) using the Kosambi mapping function (Kosambi 1943). Linkage maps were exported in the R/qtl environment (Broman et al. 2003) where they were corrected for tight double crossing-overs with the calc.errorlod function based on a LOD cutoff threshold of 2 and 1.4 for Cross #1 and Cross #2, respectively. Sex QTL detection was performed with the scanone function using a binary trait model and the EM algorithm.

Population Genomic Analyses

Brelsford and colleagues recently demonstrated how ddRADseq can be used to identify homomorphic sex

chromosomes from wild-caught adults in nonmodel animals (Brelsford et al. 2017). Because males and females share the X chromosome, a maximum allele difference of 0.5 between males and females is expected when different alleles are fixed on X and Y chromosomes. In such a case, excess heterozygosity should also be observed in males when compared with females (Brelsford et al. 2017). We used this approach to assess the extent to which chromosome 1 in unrelated wild *Ae. aegypti* populations shows enrichment for sex-differentiated markers when compared with the other two chromosomes.

RAD tags were selected that were 1) shared between $\geq 75\%$ of all individuals (males and females combined) in each *Ae. aegypti* population, and 2) had SNPs with a minor allele frequency $\geq 10\%$. Allelic difference between females and males from a population was estimated as the Weir and Cockerham F_{ST} statistic (Weir and Cockerham 1984). F_{ST} reaches a value of 0.5 for fully sex-linked markers that have alternatively fixed alleles on X and Y chromosomes. Genepop (Rousset 2008) was used to estimate F_{ST} and the frequency of heterozygotes (H) for each marker (supplementary file 2A, Supplementary Material online).

To assess if X and Y chromosomes are sufficiently differentiated to predict phenotypic sex in *Ae. aegypti*, a multivariate clustering method called discriminant analysis of principal components (DAPC) (Jombart et al. 2010) was used in the R package “adegenet” (Jombart and Ahmed 2011). DAPC was performed separately for each population and chromosome. A discriminant function was constructed for each population to distinguish males from females, using only five retained PCs in order to avoid model over fitting (Jombart and Collins 2015). Given that DAPC finds linear combinations of allele frequencies (the discriminant functions) which best separate the clusters, sex-linked markers can be identified as those with the highest allelic contribution to the discrimination of males and females.

In addition to the wild-caught *Ae. aegypti*, genome-wide differentiation patterns between males and females from the Liverpool strain were also analyzed. This inbred line originates from West Africa and has been maintained in the laboratory since 1936 (<https://www.vectorbase.org/organisms/aedes-aegypti/liverpool>; last accessed August 19, 2017). The Liverpool strain was used to generate the reference genome sequence of *Ae. aegypti* (Nene et al. 2007) as well as several partial assemblies, and remains the most commonly used material in various laboratory studies of *Ae. aegypti*. This analysis used the WGS data set generated by Hall et al. (2014). Briefly, they isolated genomic DNA separately from ten males and six virgin females from the Liverpool strain. A pooled WGS library for each sex was sequenced in paired-end on an Illumina HiSeq 1000 platform using a 100-cycle chemistry (NCBI SRA accession number SRP023515). Raw reads were processed and those with a quality score > 25 were aligned to the reference genome using the bash script pipeline and Bowtie

parameters described above. Uniquely aligned reads were further processed and analyzed using the Pooling2 pipeline (Kofler et al. 2011) to estimate allele frequencies from a pooled sequencing experiment. The Weir and Cockerham F_{ST} statistic (Weir and Cockerham 1984) between males and females was calculated for each SNP with a depth of coverage between 50 and 200 reads.

Results

We first calculated linkage map positions of 363 ddRADseq markers that were unambiguously ordered according to their physical position on the three linkage groups using 22 F_2 males and 22 F_2 females from Cross #1. The three linkage groups contained 122, 49, and 192 markers, covering 128.8, 947.6, and 232.9 cM for chromosomes 1, 2, and 3, respectively. The average spacing between markers for chromosomes 1, 2, and 3 was 1.1, 19.7, and 1.2 cM, respectively. A second linkage map spanning 129.7 cM was generated using 197 F_2 females from Cross #2. Only female mosquitoes were genotyped in this cross because it was originally designed to map quantitative trait loci (QTL) underlying dengue vector competence, a female-specific trait. Owing to the lack of genotyped males in the F_2 progeny and the sex-specific genotype segregation patterns (described below), it was not possible to obtain a linkage map for chromosome 1. The Cross #2 linkage map contained 61 and 77 markers with an average spacing between markers of 0.8 and 1.1 cM for chromosome 2 and 3, respectively (supplementary table 1, Supplementary Material online).

Across both of our linkage maps generated using the ddRADseq markers, a total of 372 unique supercontigs were assigned to the three *Ae. aegypti* chromosomes (supplementary file 2B, Supplementary Material online), representing 39.6% of the base pairs from the current reference genome sequence. Linkage group assignments of supercontigs were generally in agreement with a previously published chromosome map (Timoshevskiy et al. 2013; Juneja et al. 2014) (fig. 1). Only ten supercontigs (2.7% of all our mapped supercontigs) were assigned to different chromosomes by our linkage maps and by the published chromosome map (fig. 1). These conflicting supercontig assignments were due to misassemblies that were subsequently corrected in the recently released AeGL4 genome-wide assembly (Dudchenko et al. 2017).

Intercrosses Reveal Reduced Male Recombination along a Large Region of Chromosome 1

Recombination rates were estimated by comparing the genetic distances of the linkage maps with the AeGL4 physical genomic coordinates (supplementary fig. 1, Supplementary Material online). Average recombination rate across all

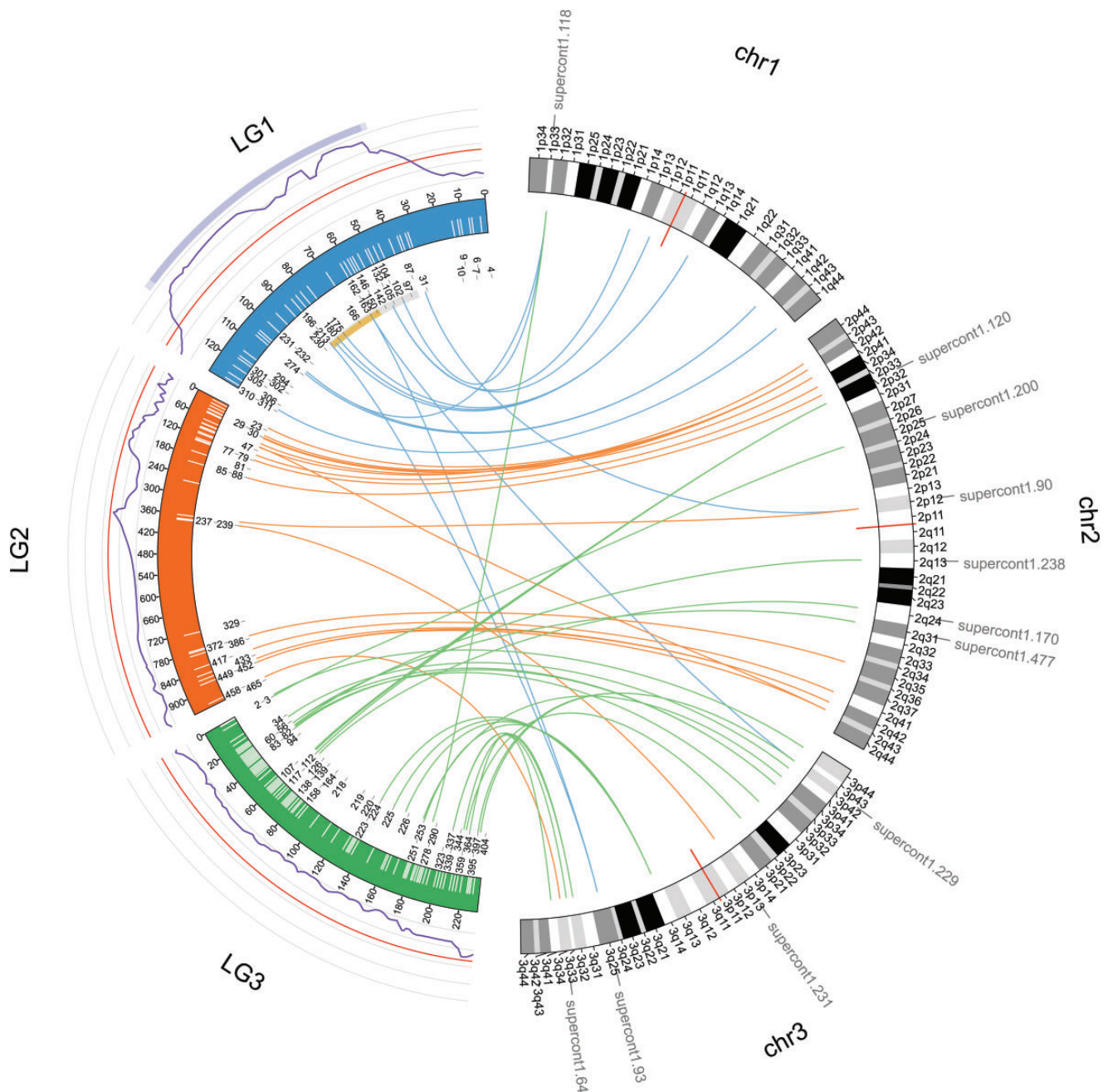


Fig. 1.—Synteny between Cross #1 linkage map and chromosome idiograms of the *Aedes aegypti* genome. Circos plot (Krzyszewski et al. 2009) shows syntenic links between linkage (left) and chromosome (right) maps. Linkage groups (LG) are 1 (blue), 2 (orange), and 3 (green). Markers are displayed with white internal ticks with position (cM) on the scale. The genetic length of LG2 is over-inflated likely due to strongly distorted genotype segregation ratios in the centromeric part. Physical marker positions in Mbp refer to the AeagL4 assembly coordinates and are represented below the linkage map. The LOD curve for the sex QTL is displayed in purple in the outer track of the linkage map, with the red line representing the genome-wide statistical significance threshold. LOD of 1.5 (dark purple) and 2 (light purple) support intervals are on the top. Centromeres are indicated with red ticks on the chromosome idiograms. Supercontigs with conflicting locations between the genetic and the chromosome maps are shown in grey next to the chromosome map. The 63-Mbp genomic region displaying high male–female genetic differentiation in the population data is delineated with a gold strip below LG1. The 123-Mbp region with undetectable recombination between X and Y chromosomes in both intercrosses is represented by the gold and the grey strips combined.

chromosomes was 0.90 cM/Mbp and 0.42 cM/Mbp for Cross #1 (chromosomes 1 and 3) and Cross #2 (chromosomes 2 and 3), respectively. These estimates are consistent with previously

published linkage maps of the *Ae. aegypti* genome (Juneja et al. 2014; Bonin et al. 2015). Because sex-specific recombination rates cannot be estimated with an F_2 intercross design,

our recombination rate estimates reflect sex-averaged recombination. However, sex-specific deviations from Mendelian segregation ratios allowed us to detect sex-specific patterns of recombination in our F_2 intercrosses.

Using a small F_2 intercross with 22 F_2 males and 22 F_2 females (Cross #1), we observed significant deviations from the expected 1:2:1 segregation ratio for sections of chromosomes 1 and 2, but only chromosome 1 contained a set of markers with a sex-specific pattern of segregation (supplementary file 2B, Supplementary Material online). Namely, a 187-Mbp region of chromosome 1 spanning from 87 Mbp (37 cM) to 274 Mbp (107 cM) showed a complete lack of F_0 paternal AA genotypes in all 22 F_2 females, and a complete lack of F_0 maternal BB genotypes in all 22 F_2 males (fig. 2B and C). This deviation from Mendelian segregation ratios is expected in the SDR because markers in perfect sex linkage cosegregate with the sex-determining locus during meiosis in F_1 males. For partially sex-linked markers, F_0 paternal A alleles preferentially segregate in F_2 males and F_0 maternal B alleles preferentially segregate in F_2 females (supplementary file 1D, Supplementary Material online). Interestingly, for one marker of this region located at position 166482560 bp in the AaegL4 assembly, there was a complete absence of AB heterozygotes and 42% and 58% of BB and AA homozygotes, respectively (fig. 2B). Such genotype proportions are consistent with the presence of a null allele on the Y chromosome, so that F_2 males that inherited the F_0 maternal B allele from their F_1 mother were erroneously genotyped as BB homozygotes instead of AB heterozygotes. Because the probability to detect low-frequency recombinants increases with larger sample size, we further analyzed 197 F_2 females from an independent F_2 intercross (Cross #2). Again, we observed a complete absence of paternal F_0 AA genotypes in all 197 F_2 females over a 150-Mbp genomic region spanning from 61 to 211 Mbp on chromosome 1 (fig. 2D). Overall, the common region with undetectable male recombination in both Cross #1 and Cross #2 spanned 123 Mbp (from 87 to 211 Mbp).

To confirm that the region showing reduced recombination between X and Y chromosomes contains the SDR, we employed QTL mapping in Cross #1. We found a major QTL associated with sex on chromosome 1 by standard interval mapping using a binary trait model (fig. 1). The highest logarithm of odds (LOD) score for this QTL was 7.6 at 49.7 cM with a 1.5 LOD support interval spanning from 35.8 to 114.7 cM. The genome-wide LOD threshold of statistical significance (α 0.05) calculated from 1,000 permutation tests was 3.30. Based on the AaegL4 assembly, the genomic region associated with a significant LOD score ranged from 30.9 to 304.6 Mbp, which represents 88.7% of the chromosome 1 physical length. Markers located in this region had genotype frequencies that significantly deviated from the expected 1:2:1 Mendelian segregation ratio only when each sex was analyzed separately (supplementary file 2B, Supplementary Material online).

X and Y Chromosomes Are Genetically Differentiated across a Large Region in the Liverpool Strain and Wild Populations

RAD markers in samples from two field-caught *Ae. aegypti* populations and WGS markers in a sample from the Liverpool strain were ordered along the three chromosomes using the AaegL4 assembly. After retaining RAD loci that were present in both sexes (<25% missing) and polymorphic in at least one sex (minor allele frequency > 10%), the data set from the field-caught Australian population contained 2,806, 5,103 and 4,149 SNPs on chromosomes 1, 2, and 3, respectively. A total of 329 markers were unassigned to the chromosome-wide AaegL4 assembly. The field-caught Brazilian population data set contained 1,009, 1,909, and 1,601 SNPs on chromosomes 1, 2, and 3, respectively. A total of 140 markers were unassigned to the chromosome-wide AaegL4 assembly. In the Liverpool data set, after retaining variants called based on a depth of coverage > 50, we analyzed 117,124 SNPs on chromosome 1, 1,268,602 SNPs on chromosome 2, and 179,794 SNPs on chromosome 3.

In all three *Ae. aegypti* population samples, genetic differentiation (F_{ST}) between males and females was 3.4- to 7.1-fold higher on chromosome 1 than on the other two chromosomes (table 1). The F_{ST} distributions of chromosomes 2 and 3 have > 96% overlap whereas the F_{ST} distributions of chromosome 1 and chromosome 2 or 3 have < 80% overlap. Genome-wide F_{ST} between males and females in the Liverpool strain ($F_{ST} = 0.044$) was elevated in comparison with the Australian ($F_{ST} = 0.027$) and Brazilian ($F_{ST} = 0.026$) samples. This likely reflects higher variance when estimating allele frequencies from a small pool-sequencing data set (6–10 individuals) than from a larger individual-based data set (>30 individuals). Regardless of the differences in experimental protocols (pooled WGS vs. ddRADseq), sample size and geographic origin, chromosome-wide F_{ST} patterns were remarkably similar among all three samples (fig. 2E–G). High male–female genetic differentiation was observed across a 103-Mbp region of chromosome 1 spanning from about 111 to 214 Mbp, which represents about one third of its physical length. Six supercontigs within this region were previously mapped by FISH to bands 1p21, 1q11–14, 1q21, in close proximity to the M-locus position (1q21).

We also detected a highly significant excess of heterozygosity for chromosome 1 markers in males relative to females (fig. 2E–F). Average frequency of heterozygotes (H) was 0.305 and 0.379 for the Australian females and males, respectively (t -test, $P < 0.001$), and 0.312 and 0.406 for the Brazilian females and males, respectively (t -test, $P < 0.001$). Differences in heterozygosity between males and females were statistically nonsignificant for other chromosomes in both groups, except for chromosome 3 in both the Australian sample (t -test, $P = 0.030$), for which females had

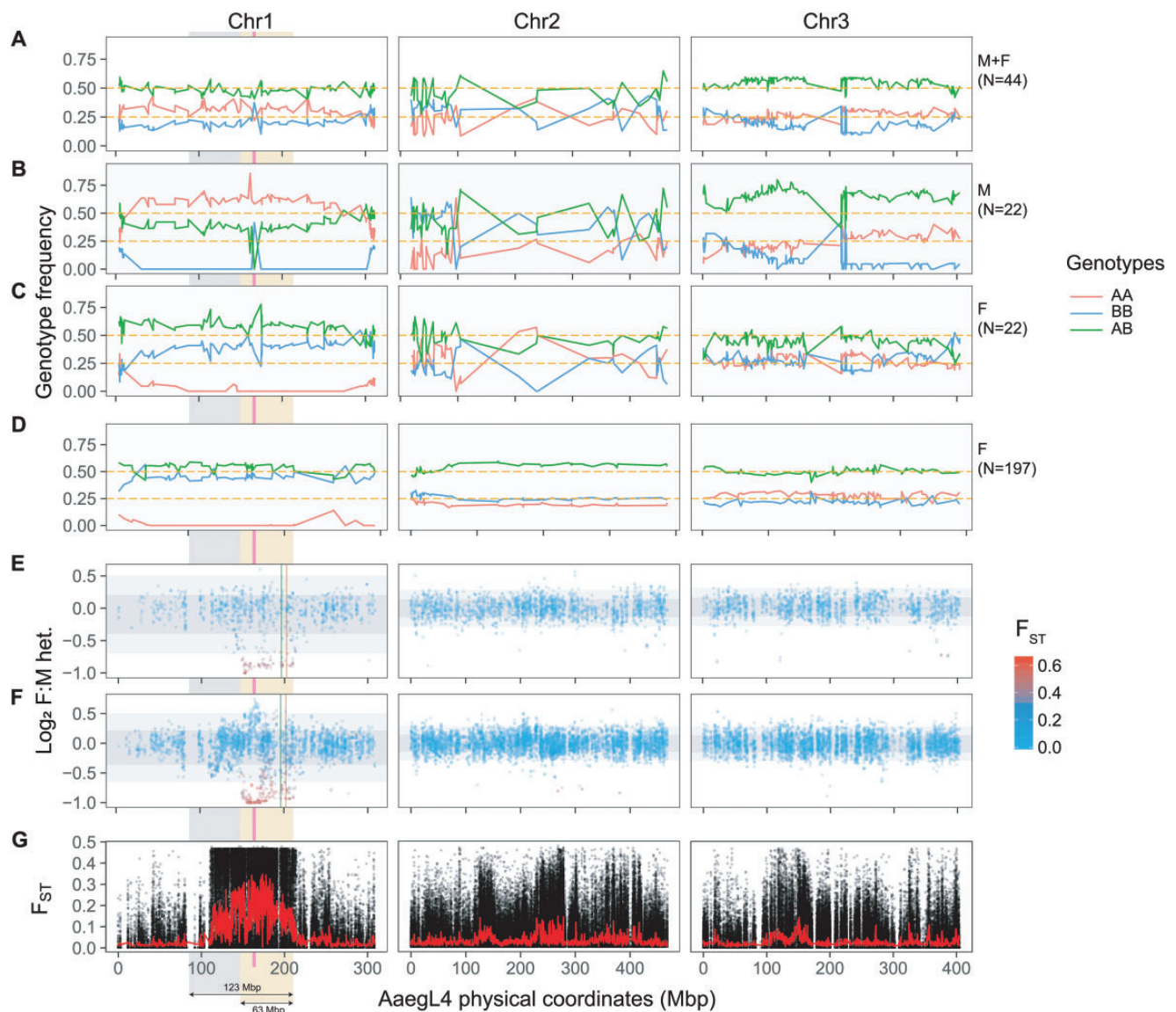


FIG. 2.—Male–female genetic differentiation and relative heterozygosity of the *Aedes aegypti* sex chromosomes. Line graphs in panels (A) through (D) represent the observed frequency of AA (red), AB (green), and BB (blue) genotypes at each marker along the three linkage groups. AA represents the F_0 paternal genotype and BB represents the F_0 maternal genotype. In Cross #1, genotype proportions of F_2 males and females together ($N = 44$), males only ($N = 22$) and females only ($N = 22$) are represented in panels (A), (B), and (C), respectively. Panel (D) represents genotype proportions for 197 females in Cross #2. Scatter plots showing \log_2 female:male heterozygosity for the Brazilian and Australian mosquito samples are displayed in panels (E) and (F), respectively, with male–female F_{ST} values (genetic differentiation) of the corresponding markers represented in a color scale. One- and two-fold standard deviations around the mean \log_2 female:male heterozygosity are displayed on each chromosome by dark and light grey strips, respectively. Green and orange vertical lines show the genomic positions of LF284T7 and LF159T7, respectively, which are two mRNA-derived sequences mapping to cytological band 1q21 where the sex-determining (M) locus is located (Timoshevskiy et al. 2013). Differentiation values calculated for the Liverpool samples (Weir and Cockerham’s F_{ST}) are displayed in panel (G) for each marker (dots) along each chromosome. The red line represents the average F_{ST} value for a 200-SNP moving window. The pink vertical line that crosses panels (B) through (F) denotes the physical position of chromosome 1 where putative null alleles were detected on the Y chromosome. The 63-Mbp genomic region displaying high male–female genetic differentiation in the population data is delineated with a gold strip below chromosome 1. The 123-Mbp region with undetectable recombination between X and Y chromosomes in both intercrosses is represented by the gold and the grey strips combined.

marginally lower heterozygosity than males, and the Brazilian sample (t -test, $P = 0.003$), for which females had higher heterozygosity than males (table 1). A 63-Mbp region of chromosome 1 spanning from 148 to 210 Mbp in the Brazilian

population and from 150 to 211 Mbp in the Australian population contained a cluster of markers with significantly higher male-to-female heterozygosity levels. The same markers showed high male–female genetic differentiation.

Table 1

Estimates of Genetic Differentiation (F_{ST}) between Females and Males, Frequency of Heterozygotes in Females (H_f) and Males (H_m), the Number Fully Sex-Linked Markers (% of the Total Number of Markers on a Given Chromosome), are Shown for Each Chromosome in Samples from Australia, Brazil, and the Liverpool Strain^a

Sample	Library Type		Chr1	Chr2	Chr3
Australia	ddRADseq	F_{ST}	0.073	0.014	0.012
		H_f	0.305	0.317	0.321
		H_m	0.379	0.316	0.329
		Sex-linked	123 (4.4%)	3 (0.06%)	1 (0.02%)
Brazil	ddRADseq	F_{ST}	0.078	0.012	0.011
		H_f	0.312	0.301	0.322
		H_m	0.406	0.302	0.305
		Sex-linked	79 (7.8%)	1 (0.05%)	3 (0.19%)
Liverpool pooled WGS		F_{ST}	0.103	0.030	0.026
		Sex-linked	7850 (7.6%)	150 (0.06%)	132 (0.08%)

^aData sets from Australia and Brazil were generated using the double-digest RAD sequencing (ddRADseq) approach with individually barcoded individuals. The Liverpool data set was generated using whole genome sequencing on pooled samples (pooled WGS).

Interestingly, we detected a smaller region in the Australian population between 153 and 178 Mbp on chromosome 1 that contained a cluster of markers with significantly higher heterozygosity in females relative to males. This higher female-to-male heterozygosity is indicative of null alleles on the Y chromosome. This cluster of markers spans a genomic region that includes the position of a putative Y-linked null allele detected in Cross #1 (166482560 bp, fig. 2B and F).

In the nonrecombining XY chromosomal system, sex-linked markers should have Weir and Cockerham's F_{ST} close to the maximal theoretical value of 0.5 and be homozygous in females and heterozygous in males (Brelsford et al. 2017). Such markers were significantly more frequent on chromosome 1 when compared with the other two chromosomes (χ^2 test, $P < 0.001$). Namely, markers with F_{ST} close to 0.5 that are homozygous in females and heterozygous in males comprised 4.4% of all markers on chromosome 1 in the Australian sample and 7.8% in the Brazilian sample. In comparison, <0.2% were found on chromosomes 2 and 3 for both the Australian and Brazilian samples (table 1). Direct estimates of heterozygosity were not possible in the Liverpool sample because the pooled sequencing approach does not allow identification of individual genotypes. Instead, we considered that markers were sex-differentiated if they had $F_{ST} > 0.4$ (as in the Australian and Brazilian samples), if one allele was fixed in females (i.e., all females were homozygous) and if the allelic frequency was close to 0.5 in males. Using this approach, we detected 7.6% of sex-differentiated markers on chromosome 1, and 0.06% and 0.08% on chromosomes 2 and 3, respectively. Therefore, sex-differentiated markers in *Ae. aegypti* are robustly identified using different sequencing and analytical approaches (table 1).

A list of markers within the differentiated XY region from the WGS experiment (Liverpool strain) would be exhaustive, but the reduced-genome-representation (ddRADseq) data set from Australia offers insight into their location and potential effects (supplementary file 2A, Supplementary Material online). The 63-Mbp region showing high F_{ST} on chromosome 1 harbored 538 genes. A total of 95 unique genes located in this region were captured by 256 (16%) intragenic markers out of the total 1,616 markers assigned to this region. Of these 95 genes, 23 (24%) contained sex-differentiated markers (i.e., markers with $F_{ST} > 0.4$, heterozygous in males and fully homozygous in females). VectorBase contained significant differential expression data between males and females for 14 out of 23 (61%) of these genes at the pupal stage (Tomchaney et al. 2014) and 11 out of 18 (61%) of these genes at the adult stage (Dissanayake et al. 2010; Tomchaney et al. 2014) (supplementary file 2C, Supplementary Material online). No significant enrichment of differentially expressed genes between males and females was observed in this chromosome 1 region relative to the other chromosomes. In comparison, 13 out of 23 randomly selected genes from the other two chromosomes (χ^2 test, $p = 1$) were reported as differentially expressed between males and females in both studies.

Discriminant analysis of principal components performed separately for each geographic sample and chromosome showed that genetic differentiation along chromosome 1 was sufficient to assign individuals to their correct sex with 98.4% accuracy in the Australian sample and 92.4% accuracy in the Brazilian sample (fig. 3). Conversely, separation based on variation on chromosomes 2 and 3 was not better than random. Correct sex assignments were 54.8% and 45.4% for chromosome 2 and 48.4% and 51.5% for chromosome 3, in the Australian and Brazilian sample, respectively (fig. 3).

Estimating Linkage Disequilibrium with the Sex-Determining Locus

Reduced recombination between X and Y chromosomes in the vicinity of the SDR is expected to lead to high LD between loci and the sex-determining locus. Because LD between such a locus (which we will denote as *A*) and the sex-determining locus (which we will denote as *M*) cannot be estimated using the standard methods for unphased autosomal genotypes, we developed an approach based on allele frequency differences between females and males.

A natural measure of LD for our purposes is r_{MA}^2 , the square of the correlation between the allelic state at the sex-determining locus and the state at locus *A* in a sample consisting of equal numbers of X and Y chromosomes (e.g., sperm). The squared correlation is useful because we are not interested in the sign of the correlation (positive or negative) but only in its magnitude (large or small). Values of r_{MA}^2 near 1 suggest that locus *A* is in the nonrecombining SDR or

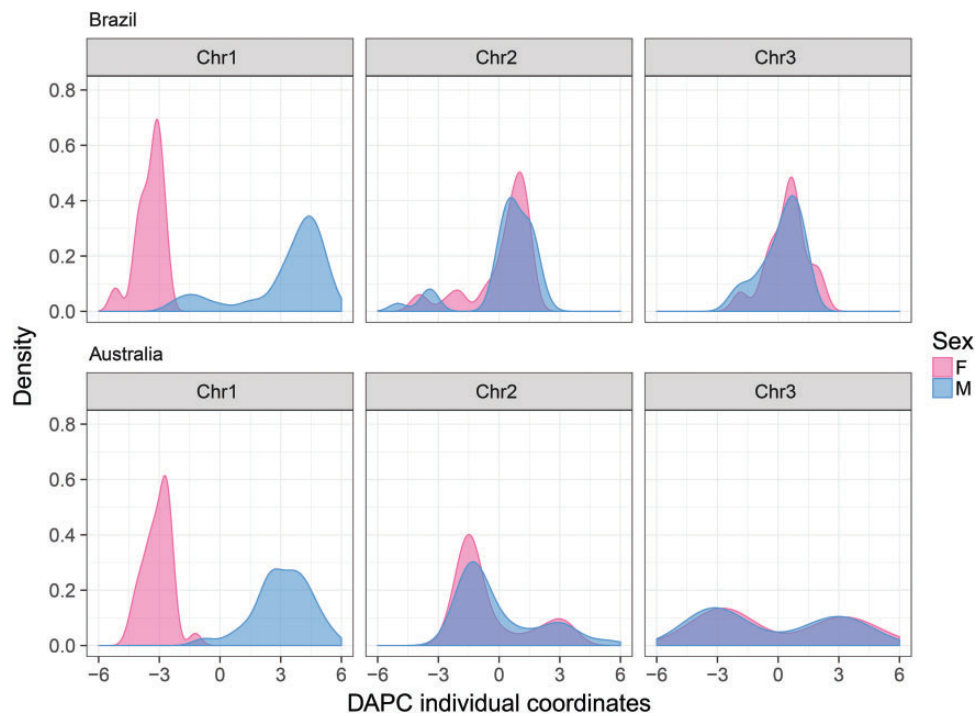


FIG. 3.—Frequency distribution of individual DAPC scores stratified by sex, for each *Aedes aegypti* chromosome and sample. DAPC accurately separates *Aedes aegypti* females from males only with chromosome 1 markers.

tightly linked to it in the pseudoautosomal region. A calculation in supplementary file 1B, Supplementary Material online shows the sample value for this statistic expressed in terms of allele frequencies at locus *A* in males and females, respectively.

We used this measure of LD with the sex-determining locus for all markers across chromosome 1 and found that markers show elevated LD with the sex-determining locus over about 103 Mbp in all three *Ae. aegypti* population data sets (supplementary fig. 2G, Supplementary Material online). Within this region there are small regions (tens of Mbp) that show lower levels of LD.

Discussion

We provide compelling evidence that the sex chromosomes of the arbovirus vector, the mosquito *Ae. aegypti*, are genetically differentiated along ~20% of their length despite the apparent homomorphy. Our findings challenge the traditional view that the homomorphic sex-determining chromosomes in *Ae. aegypti* behave like autosomes outside a small, nonrecombining SDR (referred to as the M locus in the mosquito literature). We first noticed in a small-scale F_2 intercross (Cross #1) that recombination in male meiosis was undetectable across 40% of the chromosome 1 physical length (fig. 2A–C). We next confirmed this finding in an independent F_2 intercross (Cross #2) with a larger number of individuals (fig. 2D).

Unlike a backcross design, our F_2 intercross design did not allow a direct estimation of sex-specific recombination rates. Rather, we detected sex-specific differences in recombination patterns by measuring sex-specific deviations in Mendelian inheritance. Across the three chromosomes, a single genomic region overlapping with the sex QTL on chromosome 1 showed significant sex-specific genotype segregation bias. Genotype proportions at markers located within this region significantly deviated from the expected Mendelian segregation ratio only when samples from each sex were analyzed separately. In contrast, there was no significant difference from the expected Mendelian segregation ratio for the same markers when samples were treated regardless of sex. We observed significant deviations from Mendelian inheritance on other chromosomes but they were not sex-specific (fig. 2A–C). For instance, the centromeric part of chromosome 2 contained markers that deviated from Mendelian segregation ratios and may explain its unexpectedly large genetic length. However, these non-Mendelian segregation ratios were observed regardless of sex in the F_2 progeny. Likewise, non-Mendelian segregation ratios were also observed on about half of chromosome 3 in both sexes. We speculate that sex-independent deviations from expected genotype segregation patterns on chromosomes 2 and 3 may have resulted from genetic incompatibilities between F_0 parents due to the inbreeding process.

The observation of reduced male recombination across a large portion of chromosome 1 in our mapping intercrosses

prompted us to examine patterns of molecular variation in natural populations reflecting a more ancient recombination history. In several unrelated population samples, we found a 63-Mbp region of chromosome 1 with high male-female genetic differentiation (fig. 2E–G) and high male-to-female heterozygosity (fig. 2E–F). These features are consistent with a differentiated XY chromosomal system (Brelsford et al. 2017), where homologous alleles are preferentially associated with either the X or the Y chromosome. The same 63-Mbp region contained two mRNA-derived sequences (LF284T7 and LF159T7) that mapped to cytological band 1q21, where the sex-determining locus is located (Timoshevskiy et al. 2013). The presence of Y-specific and X-specific alleles in a region of chromosome 1 that is in strong LD with the SDR (supplementary fig. 2, Supplementary Material online) is in line with the hypothesis that the non-recombining SDR might be expanding in *Ae. aegypti*. Furthermore, we identified a small cluster of markers inside the 63-Mbp region (between 153 and 178 Mbp) displaying high female-to-male heterozygosity consistent with null alleles on the Y chromosome (supplementary file 2A, Supplementary Material online). We did not observe a similar pattern in the Brazilian sample, but this could be due to the lower marker density. However, our interpretation is supported by one marker captured in Cross #1 that mapped to the same location and showed a genotype segregation pattern consistent with a null allele on the Y chromosome. A cluster of null alleles on the Y chromosome could be due to polymorphisms in the restriction enzyme cutting sites or to a deletion on the Y chromosome. Although we cannot distinguish between these two possibilities, both are in line with the sex chromosome evolution theory. Reduced recombination on the Y chromosome is predicted to weaken the efficiency of purifying selection and promote accumulation of deleterious mutations and subsequent degeneration of the Y chromosome. Further work, such as independent sequencing of the X and Y chromosomes, is required to test this hypothesis.

The 63-Mbp region of high male-female genetic differentiation in our population data was about two times smaller than the 123-Mbp region with undetectable male recombination in our intercrosses. In addition, there was lower male-female genetic differentiation on both sides of the 63-Mbp sex-differentiated genomic region. Outside of the 63-Mbp region, the female-to-male heterozygosity ratio was similar to that of chromosomes 2 and 3. This pattern could reflect suppression of recombination between the X and Y chromosomes that occurred too recently for them to have differentiated. In this case, the flanking regions would represent “evolutionary strata” analogous to those found in mammalian sex chromosomes (Lahn and Page 1999). Alternatively, the two flanking regions of the SDR may continue to recombine at a low rate, effectively preventing full differentiation between the X and Y chromosomes. Our intercrosses could have missed rare recombination events captured by the population data because of the lower number of meioses. Other

studies indicate that male recombination is not completely abolished in the vicinity of the SDR (Hall et al. 2014). Progression of homomorphic sex-determining chromosomes into heteromorphic sex chromosomes is not inevitable because examples of old homomorphic sex chromosomes exist (Charlesworth and Mank 2010; Vicoso et al. 2013a; Yazdi and Ellegren 2014; Abbott et al. 2017). Low but effective recombination rates can contribute to the maintenance of homomorphic sex chromosomes. For instance, extremely low but nonzero recombination rates between undifferentiated sex chromosomes in male tree frogs (*Hyla* spp.) were inferred from the population-based analyses of molecular variation, whereas laboratory crosses did not detect recombination (Guerrero et al. 2012). Simulation work by Grossen and colleagues showed that recombination rates as low as 10^{-4} could keep sex chromosomes homomorphic (Grossen et al. 2012).

Preservation of homomorphic sex chromosomes is generally associated with sex-biased levels of gene expression of sex-linked genes (Vicoso et al. 2013b). Evolving sex-biased gene expression could be a mechanism that alleviates selection pressure to entirely cease recombination between chromosomal regions that contain sexually antagonistic alleles (Vicoso et al. 2013; Cheng and Kirkpatrick 2016). This mechanism may provide another explanation for why sex chromosomes in *Ae. aegypti* are genetically differentiated under a level of recombination, that is, sufficient to maintain their apparent homomorphy. Perhaps mosquitoes, like birds (Vicoso et al. 2013), have found different evolutionary solutions to deal with deleterious effects of sexually antagonistic mutations. Some lineages have maintained homomorphic sex chromosomes (*Ae. aegypti* and other Culicinae), whereas others evolved heteromorphic sex chromosomes (Anophelinae). Yet, the 63-Mbp region of chromosome 1 with strong male–female differentiation was not particularly enriched with genes significantly differentially expressed between males and females at either the pupal or adult stage. Further work is required to determine whether *Ae. aegypti* homomorphic sex chromosomes are nascent heteromorphic sex chromosomes or whether evolutionary mechanisms will continue to preserve their homomorphy.

It is worth pointing out that we cannot exclude the possibility that male recombination could be reduced on all three *Ae. aegypti* chromosomes. Juneja et al. (2014) found large regions of lower recombination around the centromeres of all three chromosomes in *Ae. aegypti* females. On the other hand, dimorphism in meiotic recombination rates between sexes occurs frequently in dipterans, with individuals from the heterogametic sex usually lacking meiotic recombination. For example, this phenomenon is well known in drosophilid males (John et al. 2016). The lower male recombination that we observed in our study could therefore result from a general lack of centromeric recombination in males for all three chromosomes. In this case, the region of high LD that we

detected around the sex-determining locus may simply be the consequence of its location in the centromeric region. Under this hypothesis, the region of low recombination in chromosome 1 would not be an adaptation to the presence of a sex-determining locus, as found in many other taxa (e.g., mammals), but rather a preexisting feature of the *Ae. aegypti* genome.

It is also important to note that our analyses give conservative estimates of sequence differentiation between *Ae. aegypti* sex chromosomes because any male-specific sequences without gametologs (i.e., homologous sequences on the nonrecombining opposite sex chromosome) were not considered. Male-biased and male-specific sequences were identified as largely missing from the current genome assembly based on the Liverpool strain (Hall et al. 2014, 2015), and we detected such sequences in our ddRADseq data sets from wild populations (supplementary file 1A, Supplementary Material online). Long-read sequencing technology was recently used to improve the assembly of repeat-rich Y chromosome sequences in *Anopheles* mosquitoes (Hall et al. 2016). The same approach could be used to identify additional Y-specific sequences in *Ae. aegypti* and incorporate them into the improved genome assembly. However, thousands of putative sex-differentiated markers were detected in the WGS data set and over a hundred in the reduced genome representation (ddRADseq) data set, demonstrating that the current *Ae. aegypti* genome sequence is still informative about the sex-specific allelic variants.

Results from our intercrosses, unrelated wild populations and the most commonly used laboratory strain all point to the commonality of genetically differentiated X and Y chromosomes in *Ae. aegypti*. This means that genetic analyses involving markers on chromosome 1 should no longer assume their pseudoautosomal behavior. Linkage mapping and genome-wide association studies should implement appropriate statistical methods for sex-linked data (e.g., XWAS [Gao et al. 2015]). Population genetic analyses should check if marker deviations from the Hardy–Weinberg equilibrium stem from the nonautosomal nature of the chromosome 1 centromeric region. To date, population genetic analyses have proven challenging in *Ae. aegypti* as markers often show deviations from Hardy–Weinberg equilibrium (e.g., excess homozygosity, high LD), which can be erroneously interpreted as presence of null alleles or selection signatures. Sexes should therefore always be clearly distinguished in population genetic studies and the chromosomal location of markers should be established. Where sex separation based on morphological characters is difficult (e.g., in immature stages or damaged material), DAPC with chromosome 1 markers (fig. 3) or presence of the male-specific sequences can be used (supplementary file 1A, Supplementary Material online).

Consideration of the reduced recombination along chromosome 1 in male meiosis is also warranted for vector control strategies such as the field deployment of *Wolbachia*-infected

Ae. aegypti (Hoffmann et al. 2015). The release stocks generally undergo several generations of backcrossing with field-derived mosquitoes to create favorable combinations of alleles that increase fitness in the field as well as in the laboratory (Hoffmann et al. 2011). Because *Wolbachia* causes cytoplasmic incompatibility (Walker et al. 2011), only *Wolbachia*-infected females are crossed with males from a target field population. Lower recombination in male meiosis means that males from the release colony are expected to maintain the genetic background of the field population along a significant portion of chromosome 1.

In conclusion, our discovery of a genetically differentiated homomorphic XY chromosomal system in *Ae. aegypti* lays a new foundation for the mapping and population genetic studies in this major arbovirus vector. Extensive sex-chromosome differentiation may be exploited for accurate sexing of mosquitoes with molecular markers or provide new targets for mosquito control strategies targeting the sex-determining pathway. Our finding also calls for investigation of such chromosomal features in other Culicinae mosquitoes, many of which are significant vectors of human pathogens. Thorough understanding of sex-determination mechanisms and evolution in these mosquitoes will require improved genome assemblies that should be generated separately for each sex.

Supplementary Material

Supplementary data are available at *Genome Biology and Evolution* online.

Acknowledgments

We thank Alongkot Ponlawat, Jason Richardson, three anonymous reviewers and the Lambrechts lab members for their insights. We are grateful to Eric Deveaud, Nicolas Joly, Olivia Doppelt-Azeroual and Véronique Legrand for assistance with computational analysis, and to the Nectar Research Cloud for computational resources. The opinions or assertions contained herein are the private views of the authors and are not to be construed as reflecting the official views of the United States Army, Royal Thai Army, or the United States Department of Defense. The funders had no role in study design, data collection and interpretation, or the decision to submit the work for publication. This work was supported by Agence Nationale de la Recherche grant ANR-09-RPDOC-007-01, the French Government's Investissement d'Avenir program Laboratoire d'Excellence Integrative Biology of Emerging Infectious Diseases grant ANR-10-LABX-62-IBEID, the City of Paris Emergence(s) program in Biomedical Research, the European Union's Horizon 2020 research and innovation programme under ZikaPLAN grant agreement No 734584, Délégation Générale pour l'Armement grant No PDH-2-NRBC-4-B1-405, National Institutes of Health grant R01-GM116853, Swiss

National Science Foundation grant CRSII3-147625, The University of Melbourne Early Career Researcher grant 501152, Centre National de la Recherche Scientifique Visiting Researcher grant 1451452, and National Health and Medical Research Council program and fellowship grants.

Literature Cited

- Abbott JK, Norden AK, Hansson B. 2017. Sex chromosome evolution: historical insights and future perspectives. *Proc Biol Sci.* 284. pii: 20162806.
- Apostol BL, Black WC, Reiter P, Miller BR. 1994. Use of randomly amplified polymorphic DNA amplified by polymerase chain reaction markers to estimate the number of *Aedes aegypti* families at oviposition sites in San Juan, Puerto Rico. *Am J Trop Med Hyg.* 51(1): 89–97.
- Bachtrog D. 2013. Y-chromosome evolution: emerging insights into processes of Y-chromosome degeneration. *Nat Rev Genet.* 14(2): 113–124.
- Becker N. 2003. Mosquitoes and their control, 2nd edn. Heidelberg: Springer Verlag.
- Bonin A, et al. 2015. The genetic architecture of a complex trait: resistance to multiple toxins produced by *Bacillus thuringiensis* israelensis in the dengue and yellow fever vector, the mosquito *Aedes aegypti*. *Infect Genet Evol.* 35: 204–213.
- Bopp D, Saccone G, Beyre M. 2014. Sex determination in insects: variations on a common theme. *Sex Dev.* 8(1–3): 20–28.
- Brelsford A, Lavanchy G, Sermier R, Rausch A, Perrin N. 2017. Identifying homomorphic sex chromosomes from wild-caught adults with limited genomic resources. *Mol Ecol Res.* 17(4): 752–759.
- Broman KW, Wu H, Sen S, Churchill GA. 2003. R/qtl: QTL mapping in experimental crosses. *Bioinformatics* 19(7): 889–890.
- Catchen J, Hohenlohe PA, Bassham S, Amores A, Cresko WA. 2013. Stacks: an analysis tool set for population genomics. *Mol Ecol.* 22(11): 3124–3140.
- Catchen JM, Amores A, Hohenlohe P, Cresko W, Postlethwait JH. 2011. Stacks: building and genotyping Loci de novo from short-read sequences. *G3* 1(3): 171–182.
- Charlesworth B. 1996. The evolution of chromosomal sex determination and dosage compensation. *Curr Biol.* 6(2): 149–162.
- Charlesworth B, Charlesworth D. 2000. The degeneration of Y chromosomes. *Philos Trans R Soc Lond B Biol Sci.* 355(1403): 1563–1572.
- Charlesworth D, Mank JE. 2010. The birds and the bees and the flowers and the trees: lessons from genetic mapping of sex determination in plants and animals. *Genetics* 186(1): 9–31.
- Cheng C, Kirkpatrick M. 2016. Sex-specific selection and sex-biased gene expression in humans and flies. *PLoS Genet.* 12(9): e1006170.
- Dissanayake SN, et al. 2010. aeGEPUCI: a database of gene expression in the dengue vector mosquito, *Aedes aegypti*. *BMC Res Notes* 3: 248.
- Dudchenko O, et al. 2017. De novo assembly of the *Aedes aegypti* genome using Hi-C yields chromosome-length scaffold. *Science* 356(6333): 92–95.
- Eckermann KN, et al. 2014. Perspective on the combined use of an independent transgenic sexing and a multifactorial reproductive sterility system to avoid resistance development against transgenic Sterile Insect Technique approaches. *BMC Genet.* 15(Suppl 2): S17.
- Fansiri T, et al. 2013. Genetic mapping of specific interactions between *Aedes aegypti* mosquitoes and dengue viruses. *PLoS Genet.* 9(8): e1003621.
- Gao F, et al. 2015. XWAS: A software toolset for genetic data analysis and association studies of the X chromosome. *J Hered.* 106(5): 666–671.
- Gilles JR, et al. 2014. Towards mosquito sterile insect technique programmes: exploring genetic, molecular, mechanical and behavioural methods of sex separation in mosquitoes. *Acta Trop.* 132(Suppl): S178–S187.
- Guerrero RF, Kirkpatrick M, Perrin N. 2012. Cryptic recombination in the ever-young sex chromosomes of Hylid frogs. *J Evol Biol.* 25(10): 1947–1954.
- Hall AB, et al. 2015. A male-determining factor in the mosquito *Aedes aegypti*. *Science* 348(6240): 1268–1270.
- Hall AB, et al. 2016. Radical remodeling of the Y chromosome in a recent radiation of malaria mosquitoes. *Proc Natl Acad Sci U S A.* 113(15): E2114–E2123.
- Hall AB, et al. 2014. Insights into the preservation of the homomorphic sex-determining chromosome of *Aedes aegypti* from the discovery of a male-biased gene tightly linked to the M-locus. *Genome Biol Evol.* 6(1): 179–191.
- Hoffmann AA, et al. 2011. Successful establishment of *Wolbachia* in *Aedes* populations to suppress dengue transmission. *Nature* 476(7361): 454–457.
- Hoffmann AA, Ross PA, Rašić G. 2015. *Wolbachia* strains for disease control: ecological and evolutionary considerations. *Evol Appl.* 8(8): 751–768.
- John A, Vinayan K, Varghese J. 2016. Achiasmy: male fruit flies are not ready to mix. *Front Cell Dev Biol.* 4: 75.
- Jombart T, Ahmed I. 2011. adegenet 1.3-1: new tools for the analysis of genome-wide SNP data. *Bioinformatics* 27(21): 3070–3071.
- Jombart T, Collins C. 2015. A tutorial for Discriminant Analysis of Principal Components (DAPC) using adegenet 2.0.0. Available from: <http://adegenet.r-forge.r-project.org/files/tutorial-dapc.pdf>, last accessed February 2, 2016.
- Jombart T, Devillard S, Balloux F. 2010. Discriminant analysis of principal components: a new method for the analysis of genetically structured populations. *BMC Genet.* 11: 94.
- Juneja P, et al. 2014. Assembly of the genome of the disease vector *Aedes aegypti* onto a genetic linkage map allows mapping of genes affecting disease transmission. *PLoS Negl Trop Dis.* 8(1): e2652.
- Kaiser VB, Bachtrog D. 2010. Evolution of sex chromosomes in insects. *Annu Rev Genet.* 44: 91–112.
- Kofler R, Pandey RV, Schlötterer C. 2011. PoPoolation2: identifying differentiation between populations using sequencing of pooled DNA samples (Pool-Seq). *Bioinformatics* 27(24): 3435–3436.
- Kosambi DD. 1943. The estimation of map distances from recombination values. *Ann Eugen.* 12(1): 172–175.
- Krzywinski M, et al. 2009. Circos: an information aesthetic for comparative genomics. *Genome Res.* 19(9): 1639–1645.
- Lahn BT, Page DC. 1999. Four evolutionary strata on the human X chromosome. *Science* 286(5441): 964–967.
- Langmead B, Trapnell C, Pop M, Salzberg SL. 2009. Ultrafast and memory-efficient alignment of short DNA sequences to the human genome. *Genome Biol.* 10(3): R25.
- Margarido GR, Souza AP, Garcia AA. 2007. OneMap: software for genetic mapping in outcrossing species. *Hereditas* 144(3): 78–79.
- Motara MA, Rai KS. 1978. Giemsa C-banding patterns in *Aedes* (*Stegomyia*) mosquitoes. *Chromosoma* 70(1): 51–58.
- Nene V, et al. 2007. Genome sequence of *Aedes aegypti*, a major arbovirus vector. *Science* 316(5832): 1718–1723.
- Peterson BK, Weber JN, Kay EH, Fisher HS, Hoekstra HE. 2012. Double digest RADseq: an inexpensive method for de novo SNP discovery and genotyping in model and non-model species. *PLoS One* 7(5): e37135.
- Rašić G, et al. 2016. The queenslandensis and the type form of the Dengue Fever Mosquito (*Aedes aegypti* L.) Are Genomically Indistinguishable. *PLoS Negl Trop Dis.* 10(11): e0005096.
- Rasic G, Filipovic I, Weeks AR, Hoffmann AA. 2014. Genome-wide SNPs lead to strong signals of geographic structure and relatedness patterns in the major arbovirus vector, *Aedes aegypti*. *BMC Genomics* 15: 275.
- Rašić G, et al. 2015. Contrasting genetic structure between mitochondrial and nuclear markers in the dengue fever mosquito from Rio de Janeiro: implications for vector control. *Evol Appl.* 8(9): 901–915.

- Rice WR. 1987. The accumulation of sexually antagonistic genes as a selective agent promoting the evolution of reduced recombination between primitive sex chromosomes. *Evolution* 41(4): 911–914.
- Rousset F. 2008. genepop'007: a complete re-implementation of the genepop software for Windows and Linux. *Mol Ecol Res.* 8(1): 103–106.
- Salz HK. 2011. Sex determination in insects: a binary decision based on alternative splicing. *Curr Opin Genet Dev.* 21(4): 395–400.
- Timoshevskiy VA, et al. 2014. Genomic composition and evolution of *Aedes aegypti* chromosomes revealed by the analysis of physically mapped supercontigs. *BMC Biol.* 12(1): 1–13.
- Timoshevskiy VA, et al. 2013. An integrated linkage, chromosome, and genome map for the yellow fever mosquito *Aedes aegypti*. *PLoS Negl Trop Dis.* 7(2): e2052.
- Tomchaney M, et al. 2014. Examination of the genetic basis for sexual dimorphism in the *Aedes aegypti* (dengue vector mosquito) pupal brain. *Biol Sex Differ.* 5: 10.
- Toups MA, Hahn MW. 2010. Retrogenes reveal the direction of sex-chromosome evolution in mosquitoes. *Genetics* 186(2): 763–766.
- Vicoso B, Bachtrog D. 2015. Numerous transitions of sex chromosomes in Diptera. *PLoS Biol.* 13(4): e1002078.
- Vicoso B, et al. 2013a. Comparative sex chromosome genomics in snakes: differentiation, evolutionary strata, and lack of global dosage compensation. *PLoS Biol.* 11(8): e1001643.
- Vicoso B, Kaiser VB, Bachtrog D. 2013. Sex-biased gene expression at homomorphic sex chromosomes in emus and its implication for sex chromosome evolution. *Proc Natl Acad Sci U S A.* 110(16): 6453–6458.
- Walker T, et al. 2011. The wMel Wolbachia strain blocks dengue and invades caged *Aedes aegypti* populations. *Nature* 476(7361): 450–453.
- Weir BS, Cockerham CC. 1984. Estimating F-statistics for the analysis of population structure. *Evolution* 38(6): 1358–1370.
- Yazdi HP, Ellegren H. 2014. Old but not (so) degenerated: slow evolution of largely homomorphic sex chromosomes in ratites. *Mol Biol Evol.* 31(6): 1444–1453.

Associate editor: Judith Mank



Minerva Access is the Institutional Repository of The University of Melbourne

Author/s:

Fontaine, A; Filipovic, L; Fansiri, T; Hoffmann, AA; Cheng, C; Kirkpatrick, M; Rasic, G;
Lambrechts, L

Title:

Extensive Genetic Differentiation between Homomorphic Sex Chromosomes in the Mosquito
Vector, *Aedes aegypti*

Date:

2017-09-01

Citation:

Fontaine, A., Filipovic, L., Fansiri, T., Hoffmann, A. A., Cheng, C., Kirkpatrick, M., Rasic, G.
& Lambrechts, L. (2017). Extensive Genetic Differentiation between Homomorphic Sex
Chromosomes in the Mosquito Vector, *Aedes aegypti*. *GENOME BIOLOGY AND
EVOLUTION*, 9 (9), pp.2322-2335. <https://doi.org/10.1093/gbe/evx171>.

Persistent Link:

<http://hdl.handle.net/11343/257154>

File Description:

published version

License:

CC BY-NC